

OPTIMISATION OF A PERMANENT MAGNET MULTI-ENERGY FFA ARC FOR THE CEBAF ENERGY UPGRADE*

S.J. Brooks[†], Brookhaven National Laboratory, Upton, NY, USA

Abstract

It is currently planned to increase the energy of the CEBAF recirculating linear accelerator to 20 GeV or more by adding two new recirculating arcs that contain multiple new energy passes. The beam is continuous (CW), so no field ramping is desired, making this a fixed-field accelerator (FFA). The wide energy range requires a low dispersion lattice that can be created with high-gradient permanent magnets. One constraint is the existing tunnel radius in relation to the fields achievable by practically-sized permanent magnets. Thus, searching for the most efficient implementation in terms of magnet material volume is important. In this paper, a lattice cell search and optimisation is conducted that evaluates cells by the magnet volume per unit length, with the permanent magnet designs also produced via an automated code. The new lattice cells are compared to the previous manually designed cell.

LATTICE CONSTRAINTS

The fixed-field (FFA) arcs of the CEBAF energy upgrade [1, 2] will replace the final electromagnetic arcs of the current 12 GeV CEBAF but allow a wide energy range to be transmitted. For the east arc studied in this paper, this range will be approximately 10.5–21 GeV. Option A in Table 1 is the baseline as of December 2022, which is a linear field FFA. All lattices in this study have the simple structure **BD o BF o** where **o** is a drift space.

Table 1: Lattice Option Design Rules

Option	Energy (GeV)		Cell tune (cycles)	
	Min.	Max.	Min.	Max.
A	10.494	21.014	0.0363*	0.3943*
B	10.494	21.014	0.035	0.4
C	10.494	21.014	0.035	0.4
D	9	21	0.04	0.39
E	9	21	0.05	0.32

Option	Max. Dipole (T)	Gradient (T/m)	Sextupole (T/m ²)
A	1.2815*	43.44*	0
B	2	100	0
C	2	100	2000
D	2	100	400
E	2	100	400

* Point design values, rather than optimisation limits.

* Work supported by Brookhaven Science Associates, LLC under Contract No. DE-SC0012704 with the U.S. Department of Energy.

[†] sbrooks@bnl.gov

Lines B–E of Table 1 give constraints for coupled lattice–magnet optimisations that otherwise try to reduce permanent magnet volume. Option B is a re-optimisation for minimum magnet volume while keeping the same energy and tune ranges. Option C allows a (potentially large) amount of sextupole to be added to the magnets, this flexibility potentially reducing magnet size further, while otherwise preserving the conditions of B. Options D and E attempt to use the additional flexibility provided by the sextupole to give an extended lower energy range, which is important for fine-tuning the facility beam energy, or dealing with other situations where the SRF linac energy gain is reduced and the beam enters the FFA arcs at below nominal energy. Option E tries a narrower cell tune range avoiding the $Q = 1/3$ resonance that could be excited by sextupoles.

Lattice cells must also conform to the 80.6 m CEBAF tunnel radius. This is enforced by setting magnet bend angles $\theta_m = (L_{\text{cell}}/80.6 \text{ m})L_m/(L_{\text{BF}} + L_{\text{BD}})$ where L_m is the magnet length, which is allowed to vary. The drift spaces are set to a constant 9 cm in optimisations B–E.

Magnet Alignment Details

Long permanent magnets are generally built in rectangular sections rather than sectors. The magnet bend angle θ is therefore implemented (in the layout reference line) as two corners of angle $\theta/2$ at either end of the magnet, with straight lines in between. A soft-edged fringe field proportional to $\frac{1}{2} + \frac{1}{2} \tanh(z/(2.5 \text{ cm}))$ is used at both ends of all magnets. To deal with orbit curvature within the magnets, they are split into six longitudinal sections, each individually centred on the range of beam orbits.

OPTIMISATION METHOD

Candidate lattice cells were tracked with the Muon1 code [3] and optimised with its built-in genetic algorithm. The optimiser started from random designs with no manually-set starting point, so the following scoring ranges were used to guide it towards viable designs.

1. If the first energy is unstable or has an unacceptable tune, the cell is scored by how far $\cos \phi$ (calculated from the trace of the transfer matrix) deviates from the desired tune range limits, where ϕ is the phase advance.
2. If the first energy has correct tunes but later ones do not, the cell is scored by the percentage of the FFA energy range that is acceptable.
3. If all energies have correct tunes, the HalbachArea code [4] is called to attempt magnet designs. If the magnet design fails, the cell is scored by peak field in the bore of the accelerator, with lower being better.

4. If all energies have correct tunes and magnets exist, the cell is scored by the average magnet area ($\sum_{\text{Elements } e} A_e L_e$)/ $\sum_e L_e$ weighted by length through the cell, with lower being better.

MAGNET CONSTRAINTS

When 2D permanent magnet designs are generated with the HalbachArea tool [4], they use the design rules given in Table 2, which ensure there is an open midplane to allow synchrotron radiation to escape, as well as allowing enough vertical room for the beam pipe. Cross sections of the resulting magnets are shown in Fig. 4.

Table 2: Permanent Magnet Design Rules

Parameter	Value
Number of wedges	24 (12 per side)
Midplane angular gap	$\pm 12^\circ$
Vertical aperture	± 8 mm
Minimum midplane gap	± 3 mm
Material	NdFeB
Grade	N42EH
B_r (real)	1.28–1.33 T
B_{r1} (for $\mu_r = 1$ model)	1.248 T
$\mu_0 H_{cJ}$	2.9 T

The magnet geometry is made of multiple wedges around the aperture, as used in CBETA [5] and adapted in geometry for the CEBAF upgrade use case, including a recently constructed prototype [6]. The material selected is one of the highest field grades that still admits reasonably good radiation resistance judged from its H_{cJ} value, although this is also being tested experimentally at CEBAF [7].

LATTICE RESULTS

The geometries of the optimised lattice cells are given in Table 3 and the magnetic fields are given in Table 4.

Table 5 shows some performance statistics for the optimised cells. Option C has the smallest average magnet area, which is also the optimiser’s figure of merit: 48% below the baseline A. This makes sense as option C was the least constrained.

Figure 1 shows the cell tunes as a function of energies within the range. Option B has nearly identical tunes to the baseline A, with its 36% reduction in orbit excursion and 11% reduction in magnet area mainly coming from shortening the cell length from 3.15 to 2.55 m.

Figure 2 shows that the tune dependence changes radically when a large amount of sextupole is allowed. This may be a problem for the FFA orbit correction scheme, which relies on the multiple beams being linearly independent by having different tunes. This is the reason for the 400 T/m² sextupole limit used in optimisations D and E.

Figure 3 shows that a smaller amount of sextupole has a less drastic impact on the tunes. The attempt at keeping

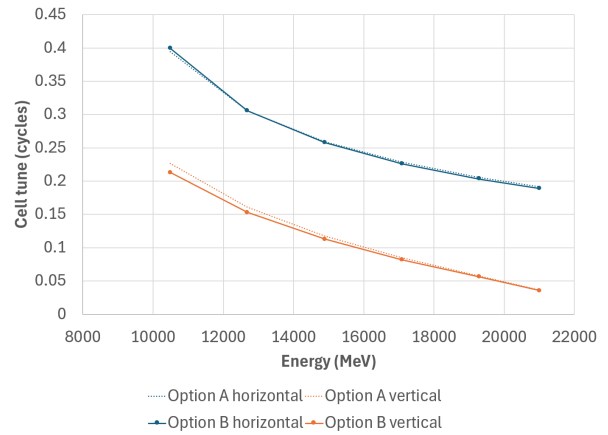


Figure 1: Cell tunes of the optimised linear field option B compared to the baseline option A.

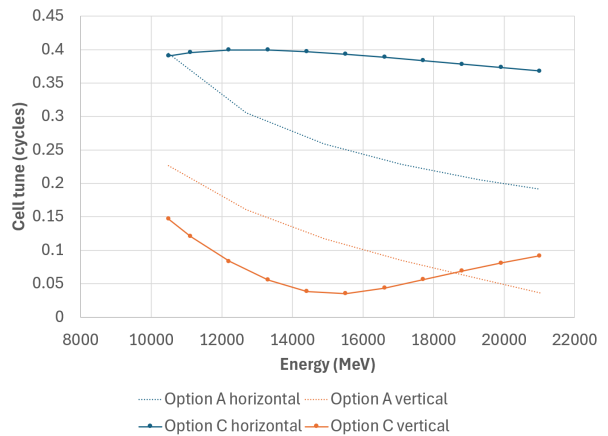


Figure 2: Cell tunes of the optimised lattice with sextupole (option C) compared to the baseline option A.

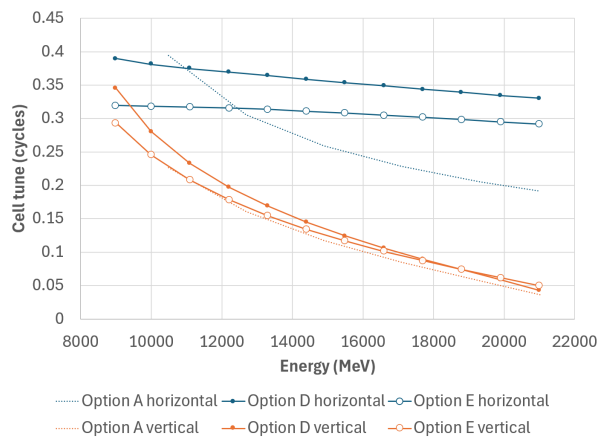


Figure 3: Cell tunes of the extended energy range sextupole lattices (D and E) compared to the baseline option A.

the tunes below 1/3 has had the side effect of making option E’s horizontal tunes nearly constant, which is bad for orbit correction. However, option D looks more reasonable.

The automatically-produced designs for all the magnets in options A–E are shown in Fig. 4.

Table 3: Lattice Geometries

Option	Lengths (m)				Angles (mrad)		
	BD	BF	Drifts	Cell	BD	BF	Cell
A	1.2448	1.6731	0.1162	3.1504	-7.11	-31.98	-39.09
B	1.1832	1.1892	0.09	2.5524	15.79	15.87	31.67
C	1.5195	1.4505	0.09	3.1500	20.00	19.09	39.08
D	1.4625	1.9760	0.09	3.6184	19.09	25.80	44.89
E	1.3814	1.7898	0.09	3.3512	18.11	23.47	41.58

Table 4: Lattice Magnetic Field Specifications

Option	Dipole (T)		Gradient (T/m)		Sextupole (T/m ²)	
	BD	BF	BD	BF	BD	BF
A	-0.3828	-1.2815	43.44	-41.13	0	0
B	0.8629	0.8629	55.155	-69.369	0	0
C	0.9590	0.9590	59.960	-89.189	-1411.41	974.97
D	0.8228	0.8228	45.345	-48.549	-400	339.94
E	0.8148	0.8148	47.548	-50.951	-400	351.95

Table 5: Lattice Results and Figures of Merit

Option	Cell tune (cycles)		$ B _{\max}$ (T)	Orbit excursion (mm)	Path length change (mm)	Magnet areas (cm ²)		
	min.	max.				Average	BD	BF
A	0.0363	0.3943	1.5346	44.968	1.233	84.69	87.43	94.41
B	0.0357	0.3994	1.6140	28.607	0.525	75.75	104.56	58.54
C	0.0352	0.3993	1.4922	23.602	0.344	44.29	59.32	34.04
D	0.0426	0.3898	1.4689	41.739	0.916	54.38	72.18	46.16
E	0.0500	0.3194	1.5438	42.966	0.910	64.24	86.07	53.86

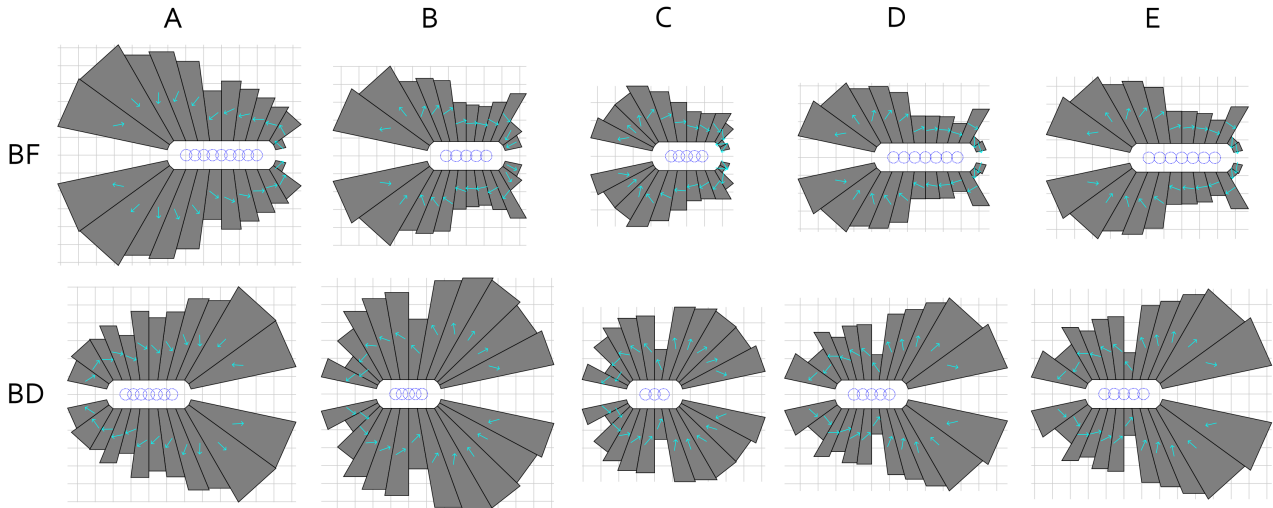


Figure 4: Cross-sections of both permanent magnets for all five lattice options. Arrows indicate magnetisation direction, grid spacing is 1 cm.

REFERENCES

- [1] K.E. Deitrick *et al.*, “CEBAF 22 GeV FFA Energy Upgrade”, Proc. IPAC 2023. doi:10.18429/JACoW-IPAC2023-MOPL182
- [2] V.S. Morozov *et al.*, “Development of FFA RLA design concept”, Proc. IPAC 2024 (this conference).
- [3] Muon1 tracking code, described in chapters 2 and 7 of S. Brooks, University of Oxford DPhil thesis “Muon capture schemes for the neutrino factory” (2010), available from <https://ora.ox.ac.uk/objects/uuid:7b724028-e4ef-4248-9d42-505e571c9e19>
- [4] S. Brooks, HalbachArea permanent magnet tool, available from <https://stephenbrooks.org/ap/halbacharea/>
- [5] S. Brooks, G. Mahler, J. Cintorino, J. Tuozzolo, and R. Michnoff, “Permanent magnets for the return loop of the Cornell-Brookhaven energy recovery linac test accelerator”, Phys. Rev. Accel. Beams **23**, 112401 (2020). doi:10.1103/PhysRevAccelBeams.23.112401
- [6] S. Brooks, “Open-Midplane Gradient Permanent Magnet with 1.53T Peak Field”, Proc. IPAC 2023. doi:10.18429/JACoW-IPAC2023-WEPM128
- [7] R.M. Bodenstein *et al.*, “Permanent Magnet Resiliency in Jefferson Lab’s Radiation Environment: LDRD Grant Status and Plan”, Proc. IPAC 2024 (this conference).